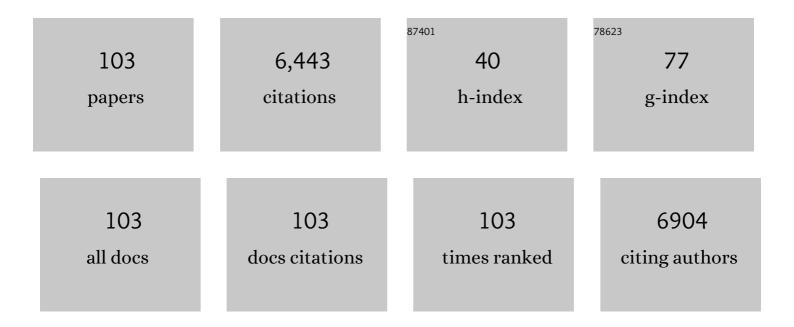
List of Publications by Year in descending order

Source: https://exaly.com/author-pdf/8450324/publications.pdf Version: 2024-02-01



Римилос 7ни

#	Article	IF	CITATIONS
1	Hydrothermal carbons/ferrihydrite heterogeneous Fenton catalysts with low H2O2 consumption and the effect of graphitization degrees. Chemosphere, 2022, 287, 131933.	4.2	21
2	A novel montmorillonite-based soil amendment for Cd/REEs immobilization and nutrients sustained release. Applied Clay Science, 2022, 221, 106464.	2.6	9
3	The different effects of sulfate on the adsorption of REEs on kaolinite and ferrihydrite. Applied Clay Science, 2022, 221, 106468.	2.6	6
4	Enhanced immobilization of phosphate by ferrihydrite during the photoreductive dissolution process. Science of the Total Environment, 2022, 838, 155835.	3.9	1
5	Coupled redox cycling of Fe and Mn in the environment: The complex interplay of solution species with Fe- and Mn-(oxyhydr)oxide crystallization and transformation. Earth-Science Reviews, 2022, 232, 104105.	4.0	25
6	Adsorption of phosphate and cadmium on iron (oxyhydr)oxides: A comparative study on ferrihydrite, goethite, and hematite. Geoderma, 2021, 383, 114799.	2.3	88
7	Phosphate modified magnetite@ferrihydrite as an magnetic adsorbent for Cd(II) removal from water, soil, and sediment. Science of the Total Environment, 2021, 764, 142846.	3.9	44
8	Facile synthesis of highly efficient and cost-effective photo-Fenton catalyst by ball milling commercial TiO2 and natural magnetite. Journal of Alloys and Compounds, 2021, 862, 158670.	2.8	13
9	Development of novel multifunctional adsorbent by effectively hosting both zwitterionic surfactant and hydrated ferric oxides in montmorillonite. Science of the Total Environment, 2021, 774, 144974.	3.9	6
10	Technical development of characterization methods provides insights into clay mineral-water interactions: A comprehensive review. Applied Clay Science, 2021, 206, 106088.	2.6	26
11	Insight into the effect of manganese substitution on mesoporous hollow spinel cobalt oxides for catalytic oxidation of toluene. Journal of Colloid and Interface Science, 2021, 594, 713-726.	5.0	70
12	Facile synthesis of Al/Fe bimetallic (oxyhydr)oxide-coated magnetite for efficient removal of fluoride from water. Environmental Technology (United Kingdom), 2020, 41, 2625-2636.	1.2	13
13	Functionalized layered double hydroxides for innovative applications. Materials Horizons, 2020, 7, 715-745.	6.4	171
14	A novel multifunctional adsorbent synthesized by modifying acidified organo-montmorillonite with iron hydroxides. Applied Clay Science, 2020, 185, 105420.	2.6	24
15	Layered intercalation compounds: Mechanisms, new methodologies, and advanced applications. Progress in Materials Science, 2020, 109, 100631.	16.0	66
16	Fabrication of layered double hydroxide/carbon nanomaterial for heavy metals removal. Applied Clay Science, 2020, 199, 105867.	2.6	18
17	Organoclay-derived lamellar silicon carbide/carbon composite as an ideal support for Pt nanoparticles: facile synthesis and toluene oxidation performance. Chemical Communications, 2020, 56, 9489-9492.	2.2	3
18	Role of phosphate concentration in control for phosphate removal and recovery by layered double hydroxides. Environmental Science and Pollution Research, 2020, 27, 16612-16623.	2.7	10

#	Article	IF	CITATIONS
19	Adsorption, degradation, and mineralization of emerging pollutants (pharmaceuticals and) Tj ETQq1 1 0.784314 Research, 2020, 27, 34862-34905.	rgBT /Ove 2.7	rlock 10 Tf 5 27
20	One-pot synthesis of the reduced-charge montmorillonite via molten salts treatment. Applied Clay Science, 2020, 186, 105429.	2.6	6
21	CNTs/ferrihydrite as a highly efficient heterogeneous Fenton catalyst for the degradation of bisphenol A: The important role of CNTs in accelerating Fe(III)/Fe(II) cycling. Applied Catalysis B: Environmental, 2020, 270, 118891.	10.8	152
22	One-pot synthesis of novel hierarchically porous and hydrophobic Si/SiOx composite from natural palygorskite for benzene adsorption. Chemical Engineering Journal, 2019, 378, 122131.	6.6	25
23	<i>In situ</i> synthesis of a silicon flake/nitrogen-doped graphene-like carbon composite from organoclay for high-performance lithium-ion battery anodes. Chemical Communications, 2019, 55, 2644-2647.	2.2	44
24	The significant effect of photo-catalyzed redox reactions on the immobilization of chromium by hematite. Chemical Geology, 2019, 524, 228-236.	1.4	13
25	Strategies for enhancing the heterogeneous Fenton catalytic reactivity: A review. Applied Catalysis B: Environmental, 2019, 255, 117739.	10.8	687
26	Photochemical behavior of ferrihydrite-oxalate system: Interfacial reaction mechanism and charge transfer process. Water Research, 2019, 159, 10-19.	5.3	73
27	Efficient degradation of cefotaxime by a UV+ferrihydrite/TiO ₂ +H ₂ O ₂ process: the important role of ferrihydrite in transferring photoâ€generated electrons from TiO ₂ to H ₂ O ₂ . Journal of Chemical Technology and Biotechnology. 2019. 94. 2512-2521.	1.6	9
28	Understanding the role of natural clay minerals as effective adsorbents and alternative source of rare earth elements: Adsorption operative parameters. Hydrometallurgy, 2019, 185, 149-161.	1.8	76
29	TiO2/Schwertmannite nanocomposites as superior co-catalysts in heterogeneous photo-Fenton process. Journal of Environmental Sciences, 2019, 80, 208-217.	3.2	17
30	Degradation of 2,4-dichlorophenol using palygorskite-supported bimetallic Fe/Ni nanocomposite as a heterogeneous catalyst. Applied Clay Science, 2019, 168, 276-286.	2.6	40
31	Self-templating synthesis of silicon nanorods from natural sepiolite for high-performance lithium-ion battery anodes. Journal of Materials Chemistry A, 2018, 6, 6356-6362.	5.2	67
32	Heterogeneous photo-Fenton degradation of bisphenol A over Ag/AgCl/ferrihydrite catalysts under visible light. Chemical Engineering Journal, 2018, 346, 567-577.	6.6	157
33	Catalytic degradation of Orange II in aqueous solution using diatomite-supported bimetallic Fe/Ni nanoparticles. RSC Advances, 2018, 8, 7687-7696.	1.7	29
34	Superior thermal stability of Keggin-Al 30 pillared montmorillonite: A comparative study with Keggin-Al 13 pillared montmorillonite. Microporous and Mesoporous Materials, 2018, 265, 104-111.	2.2	25
35	Pd nanoparticle-decorated Bi4O5Br2 nanosheets with enhanced visible-light photocatalytic activity for degradation of Bisphenol A. Journal of Photochemistry and Photobiology A: Chemistry, 2018, 356, 440-450.	2.0	43
36	Effect of acid activation of palygorskite on their toluene adsorption behaviors. Applied Clay Science, 2018, 159, 60-67.	2.6	83

#	Article	IF	CITATIONS
37	From natural clay minerals to porous silicon nanoparticles. Microporous and Mesoporous Materials, 2018, 260, 76-83.	2.2	18
38	Plasmonic Ag coated Zn/Ti-LDH with excellent photocatalytic activity. Applied Surface Science, 2018, 433, 458-467.	3.1	83
39	Three-dimensional Ag2O/Bi5O7I p–n heterojunction photocatalyst harnessing UV–vis–NIR broad spectrum for photodegradation of organic pollutants. Journal of Hazardous Materials, 2018, 344, 42-54.	6.5	192
40	Self-assembled ZnAl-LDH/PMo12 nano-hybrids as effective catalysts on the degradation of methyl orange under room temperature and ambient pressure. Applied Catalysis A: General, 2018, 550, 206-213.	2.2	18
41	Calcined Mg/Al-LDH for acidic wastewater treatment: Simultaneous neutralization and contaminant removal. Applied Clay Science, 2018, 153, 46-53.	2.6	39
42	Calcined Mg/Al layered double hydroxides as efficient adsorbents for polyhydroxy fullerenes. Applied Clay Science, 2018, 151, 66-72.	2.6	16
43	Adsorption of ammonium by different natural clay minerals: Characterization, kinetics and adsorption isotherms. Applied Clay Science, 2018, 159, 83-93.	2.6	218
44	Clay minerals derived nanostructured silicon with various morphology: Controlled synthesis, structural evolution, and enhanced lithium storage properties. Journal of Power Sources, 2018, 405, 61-69.	4.0	34
45	Superior adsorption of phosphate by ferrihydrite-coated and lanthanum-decorated magnetite. Journal of Colloid and Interface Science, 2018, 530, 704-713.	5.0	185
46	Visible-light Ag/AgBr/ferrihydrite catalyst with enhanced heterogeneous photo-Fenton reactivity via electron transfer from Ag/AgBr to ferrihydrite. Applied Catalysis B: Environmental, 2018, 239, 280-289.	10.8	123
47	Enhanced photocatalytic activity of Bi4Ti3O12 nanosheets by Fe3+-doping and the addition of Au nanoparticles: Photodegradation of Phenol and bisphenol A. Applied Catalysis B: Environmental, 2017, 200, 72-82.	10.8	184
48	Keggin-Al 30 pillared montmorillonite. Microporous and Mesoporous Materials, 2017, 242, 256-263.	2.2	39
49	Mechanisms for the enhanced photo-Fenton activity of ferrihydrite modified with BiVO 4 at neutral pH. Applied Catalysis B: Environmental, 2017, 212, 50-58.	10.8	182
50	Reduction removal of hexavalent chromium by zinc-substituted magnetite coupled with aqueous Fe(II) at neutral pH value. Journal of Colloid and Interface Science, 2017, 500, 20-29.	5.0	23
51	A novel synergy of Er3+/Fe3+ co-doped porous Bi5O7I microspheres with enhanced photocatalytic activity under visible-light irradiation. Applied Catalysis B: Environmental, 2017, 205, 421-432.	10.8	123
52	Influence of interlayer species on the thermal characteristics of montmorillonite. Applied Clay Science, 2017, 135, 129-135.	2.6	41
53	Converting Spent Cu/Fe Layered Double Hydroxide into Cr(VI) Reductant and Porous Carbon Material. Scientific Reports, 2017, 7, 7277.	1.6	28
54	An efficient catalyst of manganese supported on diatomite for toluene oxidation: Manganese species, catalytic performance, and structure-activity relationship. Microporous and Mesoporous Materials, 2017, 239, 101-110.	2.2	54

#	Article	IF	CITATIONS
55	Enhanced photocatalytic activity of Zn/Ti-LDH via hybridizing with C60. Molecular Catalysis, 2017, 427, 54-61.	1.0	34
56	In situ sequentially generation of acid and ferrous ions for environmental remediation. Chemical Engineering Journal, 2016, 302, 223-232.	6.6	15
57	Bisphenol A degradation by a new acidic nano zero-valent iron diatomite composite. Catalysis Science and Technology, 2016, 6, 6066-6075.	2.1	34
58	Adsorption of polyhydroxy fullerene on polyethylenimine-modified montmorillonite. Applied Clay Science, 2016, 132-133, 412-418.	2.6	19
59	Fullerol modification ferrihydrite for the degradation of acid red 18 under simulated sunlight irradiation. Journal of Molecular Catalysis A, 2016, 424, 393-401.	4.8	24
60	One-step solvothermal synthesis of Fe-doped BiOI film with enhanced photocatalytic performance. RSC Advances, 2016, 6, 106615-106624.	1.7	20
61	BiVO4/Fe/Mt composite for visible-light-driven degradation of acid red 18. Applied Clay Science, 2016, 129, 27-34.	2.6	21
62	Visible light assisted Fenton-like degradation of Orange II on Ni 3 Fe/Fe 3 O 4 magnetic catalyst prepared from spent FeNi layered double hydroxide. Journal of Molecular Catalysis A, 2016, 415, 9-16.	4.8	41
63	Adsorbents based on montmorillonite for contaminant removal from water: A review. Applied Clay Science, 2016, 123, 239-258.	2.6	389
64	Ag ₃ PO ₄ immobilized on hydroxy-metal pillared montmorillonite for the visible light driven degradation of acid red 18. Catalysis Science and Technology, 2016, 6, 4116-4123.	2.1	35
65	Efficiency of Fe–montmorillonite on the removal of Rhodamine B and hexavalent chromium from aqueous solution. Applied Clay Science, 2016, 120, 9-15.	2.6	53
66	The variation of cationic microstructure in Mn-doped spinel ferrite during calcination and its effect on formaldehyde catalytic oxidation. Journal of Hazardous Materials, 2016, 306, 305-312.	6.5	38
67	Adsorption of phenol, phosphate and Cd(II) by inorganic–organic montmorillonites: A comparative study of single and multiple solute. Colloids and Surfaces A: Physicochemical and Engineering Aspects, 2016, 497, 63-71.	2.3	43
68	Co-adsorption of phosphate and zinc(II) on the surface of ferrihydrite. Chemosphere, 2016, 144, 1148-1155.	4.2	118
69	Adsorption of phenol and Cu(II) onto cationic and zwitterionic surfactant modified montmorillonite in single and binary systems. Chemical Engineering Journal, 2016, 283, 880-888.	6.6	112
70	Effect of Mn substitution on the promoted formaldehyde oxidation over spinel ferrite: Catalyst characterization, performance and reaction mechanism. Applied Catalysis B: Environmental, 2016, 182, 476-484.	10.8	149
71	Thermal analysis evidence for the location of zwitterionic surfactant on clay minerals. Applied Clay Science, 2015, 112-113, 62-67.	2.6	27
72	Organo-Clays As Sorbents of Hydrophobic Organic Contaminants: Sorptive Characteristics and Approaches to Enhancing Sorption Capacity. Clays and Clay Minerals, 2015, 63, 199-221.	0.6	32

RUNLIANG ZHU

#	Article	IF	CITATIONS
73	Simultaneous adsorption of Cd(<scp>ii</scp>) and phosphate on Al ₁₃ pillared montmorillonite. RSC Advances, 2015, 5, 77227-77234.	1.7	39
74	Sequestration of heavy metal cations on montmorillonite by thermal treatment. Applied Clay Science, 2015, 107, 90-97.	2.6	21
75	Modelling the effects of surfactant loading level on the sorption of organic contaminants on organoclays. RSC Advances, 2015, 5, 47022-47030.	1.7	24
76	From spent Mg/Al layered double hydroxide to porous carbon materials. Journal of Hazardous Materials, 2015, 300, 572-580.	6.5	28
77	Templated synthesis of nitrogen-doped graphene-like carbon materials using spent montmorillonite. RSC Advances, 2015, 5, 7522-7528.	1.7	34
78	Investigation of structure and thermal stability of surfactant-modified Al-pillared montmorillonite. Journal of Thermal Analysis and Calorimetry, 2014, 115, 219-225.	2.0	13
79	Restricting layer collapse enhances the adsorption capacity of reduced-charge organoclays. Applied Clay Science, 2014, 88-89, 73-77.	2.6	17
80	Surface Heterogeneity of SiO ₂ Polymorphs: An XPS Investigation of α-Quartz and α-Cristobalite. Journal of Physical Chemistry C, 2014, 118, 26249-26257.	1.5	41
81	Al13-pillared montmorillonite modified by cationic and zwitterionic surfactants: A comparative study. Applied Clay Science, 2014, 101, 327-334.	2.6	13
82	Structure and dynamic properties of water saturated CTMA-montmorillonite: molecular dynamics simulations. Applied Clay Science, 2014, 97-98, 62-71.	2.6	30
83	Co-sorption of Cd and phosphate on the surface of a synthetic hydroxyiron-montmorillonite complex. Clays and Clay Minerals, 2014, 62, 79-88.	0.6	26
84	From used montmorillonite to carbon monolayer–montmorillonite nanocomposites. Applied Clay Science, 2014, 100, 112-117.	2.6	39
85	Montmorillonite as a multifunctional adsorbent can simultaneously remove crystal violet, cetyltrimethylammonium, and 2-naphthol from water. Applied Clay Science, 2014, 88-89, 33-38.	2.6	43
86	Application of linear free energy relationships to characterizing the sorptive characteristics of organic contaminants on organoclays from water. Journal of Hazardous Materials, 2012, 233-234, 228-234.	6.5	20
87	Molecular dynamics simulation of TCDD adsorption on organo-montmorillonite. Journal of Colloid and Interface Science, 2012, 377, 328-333.	5.0	34
88	Sorptive Characteristics of Organomontmorillonite toward Organic Compounds: A Combined LFERs and Molecular Dynamics Simulation Study. Environmental Science & Technology, 2011, 45, 6504-6510.	4.6	46
89	Sorption of 2,4-Dichlorophenol onto Organobentonites: Influence of Organic Cation Structure and Bentonite Layer Charge. Adsorption Science and Technology, 2011, 29, 29-38.	1.5	11
90	Structural and sorptive characteristics of the cetyltrimethylammonium and polyacrylamide modified bentonite. Chemical Engineering Journal, 2010, 160, 220-225.	6.6	28

RUNLIANG ZHU

#	Article	IF	CITATIONS
91	Removal of hexavalent chromium [Cr(VI)] from aqueous solutions by the diatomite-supported/unsupported magnetite nanoparticles. Journal of Hazardous Materials, 2010, 173, 614-621.	6.5	327
92	Enhancing the sorption capacity of CTMA-bentonite by simultaneous intercalation of cationic polyacrylamide. Journal of Hazardous Materials, 2010, 178, 1078-1084.	6.5	22
93	Regeneration of spent organoclays after the sorption of organic pollutants: A review. Journal of Environmental Management, 2009, 90, 3212-3216.	3.8	67
94	Simultaneous sorption of crystal violet and 2-naphthol to bentonite with different CECs. Journal of Hazardous Materials, 2009, 166, 195-199.	6.5	62
95	Sorption of naphthalene and phosphate to the CTMAB–Al13 intercalated bentonites. Journal of Hazardous Materials, 2009, 168, 1590-1594.	6.5	60
96	Intercalation of both CTMAB and Al13 into montmorillonite. Journal of Colloid and Interface Science, 2009, 335, 77-83.	5.0	47
97	Thermodynamics of naphthalene sorption to organoclays: Role of surfactant packing density. Journal of Colloid and Interface Science, 2008, 322, 27-32.	5.0	34
98	Structure of surfactant–clay complexes and their sorptive characteristics toward HOCs. Separation and Purification Technology, 2008, 63, 156-162.	3.9	37
99	Surface structure of CTMA+ modified bentonite and their sorptive characteristics towards organic compounds. Colloids and Surfaces A: Physicochemical and Engineering Aspects, 2008, 320, 19-24.	2.3	24
100	Microstructure of organo-bentonites in water and the effect of steric hindrance on the uptake of organic compounds. Clays and Clay Minerals, 2008, 56, 144-154.	0.6	43
101	Sorption characteristics of CTMA–bentonite complexes as controlled by surfactant packing density. Colloids and Surfaces A: Physicochemical and Engineering Aspects, 2007, 294, 221-227.	2.3	69
102	Influence of clay charge densities and surfactant loading amount on the microstructure of CTMA–montmorillonite hybrids. Colloids and Surfaces A: Physicochemical and Engineering Aspects, 2007, 304, 41-48.	2.3	69
103	Simultaneous sorption of organic compounds and phosphate to inorganic–organic bentonites from water. Separation and Purification Technology, 2007, 54, 71-76.	3.9	84